REYNOLDS-NUMBER SCALING OF TURBULENT CHANNEL FLOW

Michael P. Schultz
Department of Naval Architecture and Ocean Engineering
United States Naval Academy
Annapolis, Maryland 21402 USA
mschultz@usna.edu

Karen A. Flack
Department of Mechanical Engineering
United States Naval Academy
Annapolis, Maryland 21402 USA
flack@usna.edu

ABSTRACT

Results of an experimental study of smooth-wall, fully-developed, turbulent channel flow are presented. The Reynolds number (Re_m) based on the channel height and the bulk mean velocity ranged from 10,000 – 300,000. The present results indicate that the skin-friction coefficient (C_f) closely follows a power law for $Re_m <$ 62,000. At higher Reynolds numbers, C_f is best described by a log law. Detailed two-component velocity measurements taken at friction Reynolds numbers of $Re_\tau =$ 1,000 – 6,000 indicate that the mean flow and Reynolds shear stress display little or no Reynolds-number dependence. The streamwise Reynolds normal stress ($\overline{u'^2}^+$), on the other hand, varies significantly with Reynolds number. The inner peak in $\overline{u'^2}^+$ is observed to grow with Reynolds number. Growth in $\overline{u'^2}^+$ farther from the wall is documented over the entire range of Reynolds number giving rise to a plateau in the streamwise Reynolds normal stress in the overlap region of the profile for $Re_\tau =$ 6,000. The wall-normal Reynolds normal stress ($\overline{v'^2}^+$) displays no Reynolds-number dependence near the wall. Some increase in $\overline{v'^2}^+$ in the outer layer is noted for $Re_\tau \leq$ 4,000.

INTRODUCTION

Studies of three canonical flows form the basis for much of the understanding of wall-bounded turbulence. These include the fully-developed plane channel flow, the fully-developed pipe flow, and the zero-pressure-gradient boundary layer. Computationally, the turbulent channel flow is the most studied using direct numerical simulation (DNS) largely because of the simplicity of the boundary conditions. For this reason, fully-resolved simulations of turbulent channel flow have been carried out at friction Reynolds numbers, Re_τ, up to 2,000 (*e.g.* Hoyas and Jimenez, 2006) which far exceed the Reynolds numbers reached for either pipe or boundary layer flow simulations. However, experimental turbulence measurements for channels at high Reynolds number are rather limited and lag behind pipe and boundary layer flow studies.

Turbulent channel flow has been studied experimentally by a number of investigators (*e.g.* Laufer, 1950; Comte-Bellot, 1965; Johansson and Alfredsson, 1982; Wei and Willmarth, 1989). Much of this research has focused on the Reynolds-number dependence of the skin friction and the mean flow and is reviewed in Dean (1978). Studies of the Reynolds-number scaling of the turbulence quantities are far fewer in number. In a recent article reviewing many of the experimental studies of turbulent channel flow, Zanoun *et al*. (2009) point out that the geometrical considerations involved in achieving well resolved measurements at high Reynolds number has severely limited experimental work in this regard. For example, the combination of high aspect ratio and development length make achieving extremely high Reynolds number in a channel flow facility much more costly than for pipe or boundary layer flow. To better illustrate this, consider experimental channel and pipe flow facilities with matching height and diameter, respectfully, and the same working fluid. The high aspect ratio required for a channel flow facility to maintain nominally two-dimensional flow conditions (*i.e. W/H >* 7, where *W* is the channel width and *H* is the height (Monty, 2005)) necessitates at least an order of magnitude larger volumetric flow rate to achieve the same Reynolds number as the pipe flow facility. Because of this, the understanding of the Reynolds-number scaling behavior of the turbulent channel flow lags behind that of pipe and boundary layer flow.

Notable experimental work in turbulent channel flow includes the seminal study of Laufer (1950) which documented the streamwise turbulence statistics up to a Reynolds number based on the channel height and bulk mean velocity (Re_m) of 62,000 (friction Reynolds number, $Re_\tau \sim$ 1,500). Subsequent research by Comte-Bellot (1965) extended these measurements to $Re_m =$ 230,000 ($Re_\tau \sim$ 4,800). However, as noted by Wei and Willmarth (1989), both of these studies suffered from lack of spatial resolution. Wei and Willmarth carried out an extensive study of both the streamwise and wall-normal turbulent fluctuations using laser Doppler velocimetry (LDV). The

measurements extended to Re_m = 40,000 (Re_τ ~ 1,000). One important conclusion of this work was that the streamwise Reynolds normal stress ($\overline{u'^2}^+$) in the buffer layer increases with Reynolds number over the range of their study. This stood in contrast to previous investigations which suffered from insufficient spatial resolution and showed the opposite trend. Recent DNS studies (Hoyas and Jimenez, 2006) and experiments (Ng et al., 2011) corroborate the findings of Wei and Willmarth. However, little if any data are available to investigate the Reynolds-number scaling of streamwise turbulent flucuations at higher Reynolds number, and data on the other components of the Reynolds stress tensor are quite sparse. That is the purpose of the present work.

EXPERIMENTAL FACILITIES AND METHOD

The experiments were performed in the High Reynolds Number Turbulent Channel Flow facility at the United States Naval Academy, shown in Figure 1. The test section of the channel is 25 mm in height (H), 200 mm in width (W), and 3.1 m in length (L). This gives an aspect ratio (W/H) of 8 which according to Monty (2005) is sufficient to ensure two-dimensionality of the flow along the centerline of the channel. The facility's reservoir tank holds 4000 L of water, and the temperature of the water is held constant to within ±0.25° C via a thermostat controlled chiller unit. The water in the facility is also filtered to 1 μm and deaerated. The flow is driven by two 7.5 kW pumps which are computer controlled by separate variable frequency drive units. The pumps operate in parallel and generate a bulk mean velocity of 0.4 – 11.0 ms^{-1} in the test section. The flow rate in the facility is measured using a Yokogawa ADMAG AXF magnetic flowmeter that has an accuracy of ±0.2% of the reading. The resulting Reynolds number based on the channel height and bulk mean velocity (Re_m) ranges from 10,000 – 300,000.
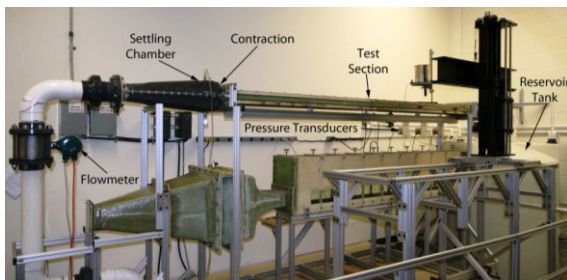
Figure 1. High Reynolds number turbulent channel flow facility at the United States Naval Academy.

The settling chamber upstream of the test section is fitted with a honeycomb flow straightener with 6 mm diameter cells, 75 mm in length. The flow then passes through a two-dimensional contraction with an 8:1 area ratio. The flow is tripped at the entrance to the test section by 1.8 mm × 1.8 mm square bars located on the top and bottom walls spanning the width of the test section. The trips provide 15% blockage which was recommended by Durst et al. (1998).

Nine pressure taps are located in this section of the channel. These are 0.75 mm holes located along the centerline of the side wall of the channel and are spaced

6.8H apart. The pressure gradient is measured using three GE-Druck LPM 9000 series differential pressure transducers with ranges of 20, 50, and 100 mbar, respectively. The transducers have an accuracy of ±0.1% of full scale. Pressure taps 5 – 8 are used to measure the streamwise pressure gradient in the channel. These are located ~90H – 110H downstream of the trip at the inlet to the channel. Glass windows on the side walls opposite pressure taps 5 and 8 allow optical access to the channel. Velocity measurements were obtained using a TSI FSA3500 two-component LDV. The LDV system utilized a custom, four-beam fiber optic probe and was operated in backscatter mode. The system also employed 2.6:1 beam expansion optics at the exit of the probe to reduce measurement volume size. Further details of the LDV system are given in Schultz and Flack (2007).

In the present study, the probe volume diameter was 45 μm. This corresponds to d^+ = 3.6 at Re_τ = 1,000 and d^+ = 21 at Re_τ = 6,000. The probe volume length was 340 μm. The velocity gradient bias correction of Durst et al. (1998) was used to correct the Reynolds stresses involving u' resulting from finite probe diameter. The present data were also corrected for velocity bias by employing standard burst transit time weighting (Buchhave et al., 1979). Fringe bias was deemed insignificant, as the beams were shifted well above a burst frequency representative of twice the freestream velocity (Edwards, 1987). Further details of the measurements are outlined in Schultz and Flack (2013). The experimental conditions for the LDV measurements are presented in Table 1.

Table 1. Experimental conditions for LDV mesurements.

Case	$\bar{U}$ (ms^{-1})	U_τ (ms^{-1})	U_{CL} (ms^{-1})	Re_m	Re_τ
Re_τ = 1,000	1.48	0.075	1.69	39,800	1,010
Re_τ = 2,000	3.13	0.145	3.48	84,300	1,960
Re_τ = 4,000	6.99	0.300	7.73	188,900	4,050
Re_τ = 6,000	10.69	0.440	11.87	286,400	5,900

Figure 2 shows the mean velocity profiles at two streamwise locations (x = 90H and 110H) for Re_τ = 2,000. Also shown for comparison are the DNS results of Hoyas and Jimenez (2006) at a similar Re_τ.
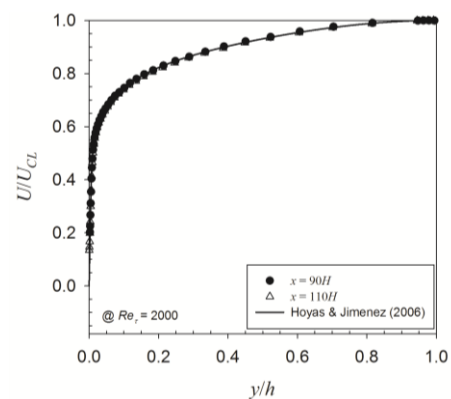
Figure 2. Mean velocity profiles at streamwise locations of x = 90H and 110H for Re_τ = 2,000 showing fully-developed flow conditions.

The collapse of the profiles from the two locations and the excellent agreement with the DNS results confirm that the flow has become fully developed over this region of the channel. Although not presented here, the higher order turbulence statistics measured at the two streamwise locations also show similar agreement.

The wall shear stress, τ_w, was determined via measurement of the streamwise pressure gradient between $90H$ and $110H$ downstream of the trip. It is given as follows

$$\tau_w = -\frac{H}{2}\frac{dp}{dx} \qquad (1)$$

or as it is more typically expressed as the skin-friction coefficient, C_f

$$C_f = \frac{\tau_w}{\frac{1}{2}\rho \overline{U}^2} = 2\left(\frac{U_\tau}{\overline{U}}\right)^2 \qquad (2)$$

where H = channel height, p = static pressure, x = streamwise distance, ρ = fluid density, $\overline{U}$ = bulk mean velocity, and U_τ = friction velocity. The development length required to achieve fully-developed conditions in terms of the streamwise pressure gradient has been a topic of significant debate as was noted in the review article of Dean (1978). In the present work, measurements indicated that the streamwise pressure gradient was constant within experimental uncertainty downstream of the first pressure tap located at $x = 63H$. This observation is supported by the recent work of Zanoun *et al.* (2009) who noted no significant variation in the streamwise pressure gradient for $x \geq 20H$.

Estimates of the overall uncertainty in the quantities presented in this work were made by combining precision and bias uncertainties using the methodology outlined in Moffat (1988). The overall uncertainty in C_f is $\pm 8.1\%$ at the lowest Reynolds number ($Re_m = 10,000$) but rapidly drops to $\pm 1.1\%$ for $Re_m \geq 40,000$. The total uncertainties in the mean flow, U, and turbulence statistics, $\overline{u'^2}$, $\overline{v'^2}$, and $-\overline{u'v'^2}$ are $\pm 1\%$, $\pm 2\%$, $\pm 3\%$, and $\pm 5\%$, respectively.

RESULTS AND DISCUSSION

The results and discussion for this study will be organized as follows. First, the skin friction in the channel will be presented. Next, the scaling of the mean flow in terms of both inner and outer variables will be given. Finally, the scaling of the Reynolds stresses in both inner and outer variables will be shown. Reynolds-number scaling will be compared to other channel flow studies as well as trends for boundary layer and pipe flows.

Skin-friction Coefficient

Figure 3 presents the skin-friction results. Here the skin-friction coefficient, C_f, is shown as a function of Reynolds number, Re_m. Also shown for comparison are the experimental results of Monty (2005) and the recent empirical correlation of Zanoun *et al.* (2009).
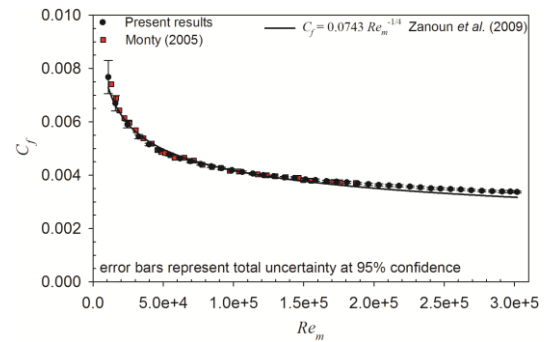
Figure 3. Skin-friction coefficient, C_f, versus Reynolds number, Re_m, for the entire range of Reynolds number investigated.

The agreement between the present results and those of Monty is within $\pm 1\%$ over the common range. The agreement with the empirical correlation proposed by Zanoun *et al.* is also within $\pm 2.5\%$ for $Re_m \leq 150,000$. At higher Reynolds numbers, the present skin-friction results are systematically larger than the power-law correlation of Zanoun *et al.*, with the difference being as much as 6% at the highest Reynolds number. The power-law form of the correlation implicitly assumes a power law in the mean velocity profile. While Zanoun *et al.* based their power-law correlation on data for $Re_m \leq 240,000$, they noted that a better fit of their higher Reynolds number data ($Re_m > 86,000$) was achieved with a logarithmic skin-friction law.

Figure 4 shows the skin-friction data presented in logarithmic form along with the logarithmic skin-friction correlation of Zanoun *et al.* (2009).
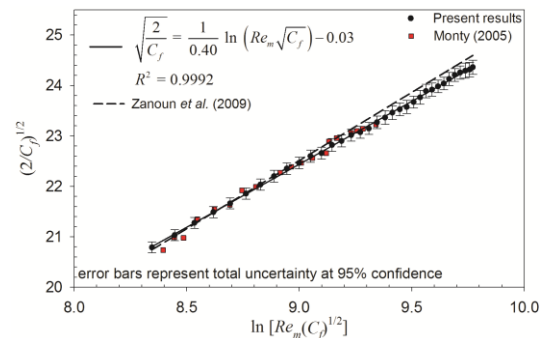
Figure 4. Skin-friction results presented in logarithmic form for $Re_m \geq 62,000$.

The present data also support the observation of Zanoun *et al.* (2009) although the emergence of a logarithmic skin-friction law appears at a slightly lower Reynolds number ($Re_m \geq 62,000$ or $Re_\tau \geq 1,500$). This corresponds to the emergence of a logarithmic law in the mean velocity profiles at these Reynolds numbers. For example, both Dean (1978) and Monty (2005) show that, following Prandtl's analysis for pipe flow, integration of the logarithmic mean velocity profile gives rise to a logarithmic skin-friction law of the form:

$$\sqrt{\frac{2}{C_f}} = C_1 \ln\left(Re_m\sqrt{C_f}\right) + C_2 \qquad (3)$$

where the constants C_1 and C_2 are directly related to the log-law constants κ, the von Karman constant, and A, the intercept, as given below.

$$C_1 = \frac{1}{\kappa} \qquad (4)$$

$$C_2 = A - \frac{1}{\kappa}\left[1 + \ln\left(2\sqrt{2}\right)\right] \qquad (5)$$

Figure 4 shows that a logarithmic skin-friction law fits the present results very well ($R^2 = 0.9992$). Within experimental uncertainty, all the data agree with the linear fit. Using this fit to the present data, yields log constants of $\kappa = 0.40$ and $A = 5.0$. Although precise determination of the log constants is not the focus of the present work, the result is worth noting. The present values are very close to the classic 'universal' values of $\kappa = 0.41$ and $A = 5.0$ given by Coles (Coles and Hirst, 1968). These constants are also in reasonable agreement with Dean's channel flow result of $\kappa = 0.41$ and $A = 5.17$. However, the present values of κ and A are higher than those reported by Zanoun *et al.* (2009) who found $\kappa = 0.369$ and $A = 3.71$ when they employed the streamwise pressure gradient to determine the wall shear stress in a turbulent channel. Recently, Marusic *et al.* (2013) proposed that the log constants are indeed universal among flow types based on analysis of high Reynolds number pipe and boundary layer data, with $\kappa = 0.39$ and $A = 4.3$. It is of note that they did not include channel flow data in their analysis likely due to the lack of such data at sufficiently high Reynolds numbers. The present results, although in reasonable agreement with the log constants of Marusic *et al.*, are nonetheless a bit higher.

Mean Flow

The mean velocity profiles are presented in inner scaling in Figure 5 for $Re_\tau = 1,000 - 6,000$. There is good collapse of the data at all Reynolds numbers over the entire inner layer indicating there is no significant Reynolds-number dependence in the mean flow in this region. The agreement between the velocity profile at $Re_\tau = 2,000$ and the results of Hoyas and Jimenez (2006) at a similar Reynolds number is also very good. DeGraaff and Eaton (2000) made a similar observation regarding the Reynolds number independence of the mean flow in the inner layer in turbulent boundary layer flow. More recently, Monty *et al.* (2009) noted remarkable similarity in the mean flow in the inner layer for turbulent boundary layer, pipe, and channel flow at $Re_\tau = 3,000$.

The outer-scaled velocity defect profiles are presented in Figure 6. These data also show excellent agreement for the mean flow in the outer layer. Again, no significant Reynolds number dependence is observed which indicates the wake is fully developed, or nearly so, for $Re_\tau \geq 1,000$. Based on the present results, the mean flow does not appear to show any Reynolds number dependence for $Re_\tau \geq 1,000$. It should be noted, however, that although the inner layer and the outer layer appear universal over this Reynolds number range, no appreciable overlap region exists for $Re_\tau = 1,000$. This agrees with the skin-friction

results (Figure 4) that indicate the emergence of a log law for $Re_\tau \geq 1,500$. As pointed out by Dean (1978) and Monty (2005), integration of a logarithmic mean profile gives rise to a log law in C_f. From this it can be inferred that a log law in the mean profile must emerge in the present work for $Re_\tau \geq 1,500$. However, close examination of the present mean flow results shows that the precise Reynolds number at which a log law region emerges and any possible Reynolds-number trend in its range are difficult to discern.
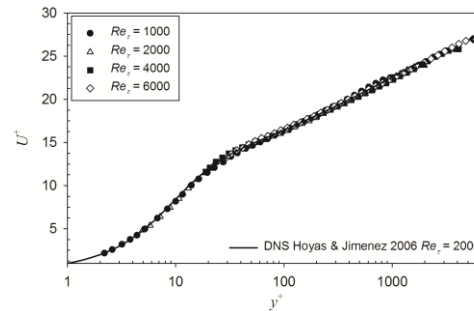
Figure 5. Mean velocity profiles in inner variables. (overall uncertainty in U^+: $\pm 1.5\%$)
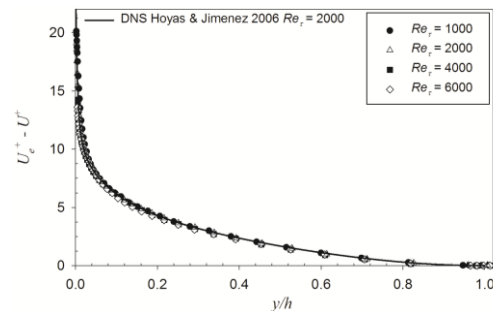
Figure 6. Mean velocity profiles in outer variables presented in velocity-defect form. (overall uncertainty in U_e^+ and U^+: $\pm 1.5\%$)

Reynolds Stresses

The inner-normalized, streamwise Reynolds stress ($\overline{u'^2}^+$) is presented in Figure 7. Shown for comparison are the DNS results of del Alamo *et al.* (2004) and Hoyas and Jimenez (2006) which correspond to the lowest two Reynolds numbers in the present study.

The agreement between the present results and the DNS is good in both cases with excellent collapse for $Re_\tau = 2,000$ case. The present data display an increase in the magnitude of inner peak with Reynolds number at least up to $Re_\tau = 4,000$. No firm conclusions can be drawn for higher Reynolds numbers as the peak is not resolved in the highest Reynolds number case. Wei and Willmarth (1989) first made this observation for the streamwise component in turbulent channel flow. However, the highest Reynolds number investigated in their study corresponds to the lowest one in the present work. A similar observation was also recently noted by Ng *et al.* (2011) for turbulent channel flow in which $Re_\tau \leq 3,000$. Qualitatively, these results also agree with the observations of DeGraaff and Eaton (2000) who noted similar trends for the zero-pressure-gradient turbulent boundary layer.
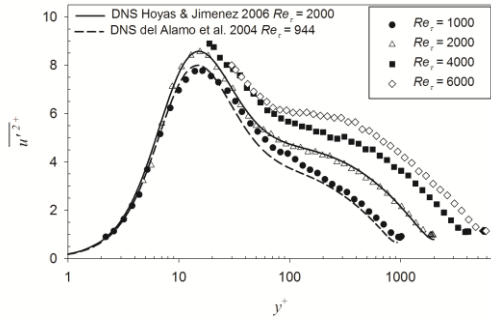
Figure 7. Streamwise Reynolds normal stress profiles in inner variables. (overall uncertainty in $\overline{u'^2}^+$: ±2.2%)

The recent results of Hultmark *et al.* (2012) for fully-developed pipe flow indicate growth in this peak is sustained for $Re_\tau \leq 3,300$, after which the value remains nearly constant at ~9, independent of Reynolds number. Monty *et al.* (2009) recently showed results for turbulent boundary layer, pipe, and channel flows at $Re_\tau = 3,000$. They observed similarity in $\overline{u'^2}^+$ in the inner layer for all three flow types. However, they noted significant differences in the u' spectra in boundary layers and those measured in pipe and channels throughout most of the flow field despite the similarity observed in $\overline{u'^2}^+$.

Also of note in the present data is an emerging plateau in $\overline{u'^2}^+$ in the log layer with increasing Reynolds number. This trend of rising $\overline{u'^2}^+$ in the outer layer is apparent in outer-normalized, streamwise Reynolds stress profiles given in Figure 8. This observation is consistent with the boundary layer results of DeGraaff and Eaton (2000) and the pipe flow results of Hultmark *et al.* (2012). However, the present Reynolds numbers are not high enough to assess if a true outer peak in $\overline{u'^2}^+$ emerges in the log layer with increasing Reynolds number as was observed in the pipe flow results of Hultmark *et al.*
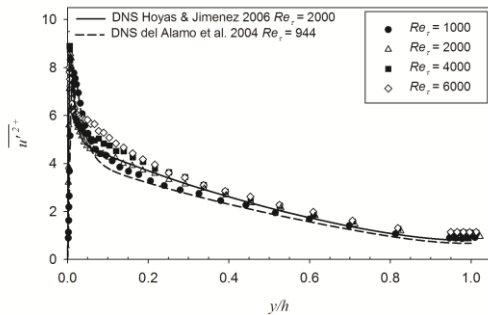
Figure 8. Streamwise Reynolds normal stress profiles in outer variables. (overall uncertainty in $\overline{u'^2}^+$: ±2.2%)

The inner-normalized, wall-normal Reynolds stress ($\overline{v'^2}^+$) is presented in Figure 9. The agreement between the present results and the DNS at similar Reynolds numbers is quite reasonable. In the near-wall region ($y^+ \leq 40$), $\overline{v'^2}^+$ does not exhibit any significant Reynolds-number dependence in contrast to what is observed in the streamwise component. The results also indicate that the maximum value of $\overline{v'^2}^+$ grows with increasing Reynolds number for $Re_\tau < 4,000$. This trend can also be clearly

seen in the outer-normalized profiles that are presented in Figure 10. For $Re_\tau \geq 4,000$, the maximum value of $\overline{v'^2}^+$ reaches a value of ~1.4 that appears to be independent of Reynolds number. The boundary layer results of DeGraaff and Eaton (2000) show a similar maximum value of $\overline{v'^2}^+$ as is observed here. However, they did not observe a clear Reynolds-number dependence in $\overline{v'^2}^+$ aside from their lowest Reynolds number case ($Re_\tau = 540$) in which $\overline{v'^2}^+$ was reduced presumably due to low Reynolds-number effects.
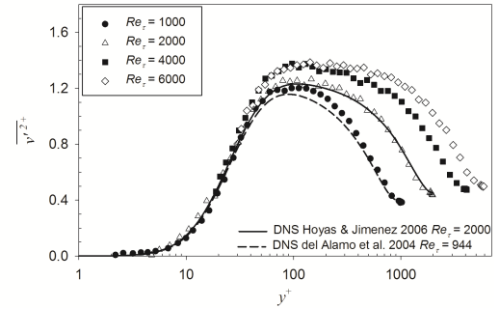
Figure 9. Wall-normal Reynolds normal stress profiles in inner variables. (overall uncertainty in $\overline{v'^2}^+$: ±3.2%)
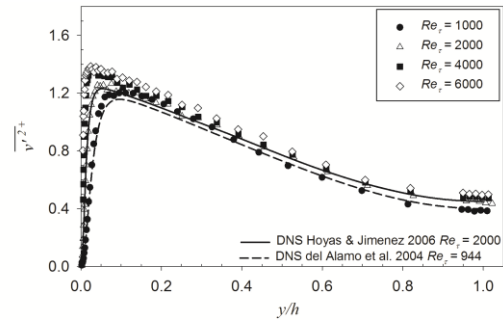
Figure 10. Wall-normal Reynolds normal stress profiles in outer variables. (overall uncertainty in $\overline{v'^2}^+$: ±3.2%)

The inner-normalized, Reynolds shear stress ($-\overline{u'v'}^+$) profiles are presented in Figure 11.
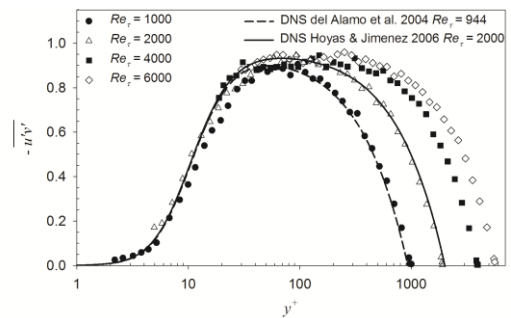
Figure 11. Reynolds shear stress profiles in inner variables. (overall uncertainty in $-\overline{u'v'}^+$: ±5.1%)

In the near-wall region ($y^+ \leq 40$), $-\overline{u'v'}^+$ behaves very similarly to $\overline{v'^2}^+$ exhibiting no Reynolds-number dependence. The outer-normalized, Reynolds shear stress profiles are presented in Figure 12. Collapse of the profiles is observed for $y/h \geq 0.1$ at all Reynolds numbers.

5

These observations agree with those of DeGraaff and Eaton (2000) for boundary layer flow. In some ways, the present observations are not surprising. The mean momentum equation and the boundary conditions in a plane channel flow require a linear decrease in the total shear stress that goes as 1-y/h. The fact that no Reynolds-number dependence was observed in the mean flow would imply that the Reynolds shear stress should also be independent of Reynolds number.
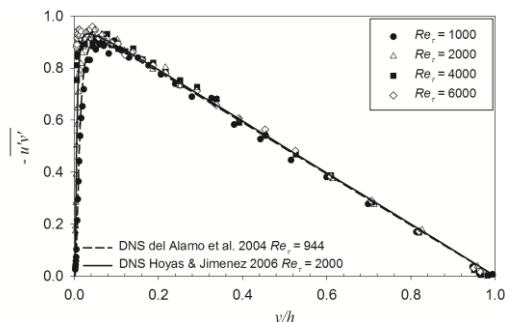
Figure 12. Reynolds shear stress profiles in outer variables. (overall uncertainty in $-\overline{u'v'}^+$: ±5.1%)

CONCLUSION

An experimental study of smooth-wall, fully-developed, turbulent channel flow has been carried out. The results indicate that the skin-friction coefficient (C_f) follows a power law for $Re_m < 60,000$, while at higher Reynolds numbers it is best characterized by a logarithmic law with $\kappa = 0.40$ and $A = 5.0$. The mean flow and Reynolds shear stress show little or no Reynolds-number dependence. However, the streamwise Reynolds normal stress ($\overline{u'^2}^+$) varies significantly with Reynolds number. The inner peak in $\overline{u'^2}^+$ is observed to grow with Reynolds number up to at least $Re_\tau = 4,000$. No conclusion can be drawn for higher Reynolds numbers as measurements close enough to the wall to resolve the peak were not possible at $Re_\tau = 6,000$. Growth in $\overline{u'^2}^+$ farther from the wall is also documented over the entire range of Reynolds number giving rise to a plateau in the streamwise Reynolds normal stress in the overlap region of the profile for $Re_\tau = 6,000$. The wall-normal Reynolds normal stress ($\overline{v'^2}^+$) displays no Reynolds-number dependence near the wall, while a modest increase in $\overline{v'^2}^+$ in the outer layer is noted for $Re_\tau \le 4,000$.

REFERENCES

Adrian, R. J., "Laser Velocimetry" in Fluid Mechanics Measurements, 1983, R. J. Goldstein, ed., Hemisphere Publishing.

Buchhave, P., George, W. K., and Lumley, J. L., 1979, "The Measurement of Turbulence with the Laser-Doppler Anemometer", *Annu. Rev. of Fluid Mech.*, Vol. 11, pp. 443-503.

Coles, D. E., and Hirst, E. A., 1968, "Compiled Data", in *Proceedings of Computation of Turbulent Boundary Layers, AFOSR-IFP Stanford Conference* Vol.II, Stanford University Thermosciences Division.

Comte-Bellot, G., 1965, "Ecoulement turbulent entre deux parois parallèles", *Publications Scientifiques et Techniques du Ministere de 1'Air* # 419.

Dean, R. B., 1978, "Reynolds Number Dependence of Skin Friction and Other Bulk Flow Variables in Two-Dimensional Rectangular Duct Flow", *Trans. ASME - J. Fluid Eng.*, Vol. 100, pp. 215-223.

del Alamo, J. C. , Jimenez, J., Zandonade, P., and Moser, R. D., 2004, "Scaling of the Energy Spectra of Turbulent Channels", *J. Fluid Mech.,* Vol. 500, pp. 135-144.

DeGraaff D. B., and Eaton, J. K., 2000, "Reynolds-Number Scaling of the Flat-Plate Turbulent Boundary Layer", *J. Fluid Mech.,*Vol. 422, pp. 319-346.

Durst, F., Fischer, M., Jovanovic, J., and Kikura, H., 1998, "Methods to Set Up and Investigate Low Reynolds Number, Fully Developed Turbulent Plane Channel Flows", *Trans. ASME - J. Fluid Eng.*, Vol. 120, pp. 496–503.

Edwards, R. V., 1987, "Report of the Special Panel on Statistical Particle Bias Problems in Laser Anemometry", *Trans. ASME - J. Fluid Eng.*, Vol. 109, pp. 89-93.

Hoyas, S., and Jimenez, J., 2006, "Scaling of the Velocity Fluctuations in Turbulent Channels up to $Re_\tau =$ 2003", *Phys. Fluids*, Vol. 18, 011702.

Hultmark, M., Vallikivi, M., Bailey, S. C. C., and Smits, A. J., 2012, "Turbulent Pipe Flow at Extreme Reynolds Numbers", *Phys. Rev. Lett.*, Vol. 108, 094501.

Johansson, A. V., and Alfredsson, P. H., 1982, "On the Structure of Turbulent Channel Flow", *J . Fluid Mech.*, Vol. 122, pp. 295-314.

Laufer, J., 1950, "Investigation of Turbulent Flow in a Two-Dimensional Channel", *NACA Tech. Note* TN2123.

Moffat, R. J., 1988, "Describing the Uncertainties in Experimental Results", *Exp. Therm. Fluid Sci.*, Vol. 1, pp. 3-17.

Monty, J. P., 2005, *Developments in Smooth Wall Turbulent Duct Flows*, Ph.D. Thesis, University of Melbourne, Melbourne, Australia.

Monty, J. P., Hutchins, N., Ng, H. G. H., Marusic, I., and Chong, M. S., 2009, "A Comparison of Turbulent Pipe, Channel and Boundary Layer Flows", *J. Fluid Mech.,* Vol. 632, pp. 431-442.

Marusic, I., Monty, J. P., Hultmark, M., and Smits, A. J., 2013, "On the Logarithmic Region in Wall Turbulence", *J. Fluid Mech.*, Vol. 716, R3.

Ng, H. C. H., Monty, J. P., Hutchins, N., Chong, M. S. and Marusic, I., 2011, "Comparison of Turbulent Channel and Pipe Flows with Varying Reynolds Number", *Exps. Fluids*, Vol. 51, pp. 1261-1281.

Schultz, M. P. and Flack, K. A., 2007, "The Rough-Wall Turbulent Boundary Layer from the Hydraulically Smooth to the Fully Rough Regime", *J . Fluid Mech.*, Vol. 580, pp. 381-405.

Schultz, M. P. and Flack, K. A., 2013, "Reynolds-Number Scaling of Turbulent Channel Flow", *Phys. Fluids*, Vol. 25, 025104.

Wei, T., and Willmarth, W. W., 1989, "Reynolds-Number Effects on the Structure of a Turbulent Channel Flow", *J. Fluid Mech.*, Vol. 204, pp. 57-95.

Zanoun, E.-S., Nagib, H., and Durst, F., 2009, "Refined c_f Relation for Turbulent Channels and Consequences for High-Re Experiments", *Fluid Dyn. Res.*, Vol. 41, 021405.